CHAPTER 3

OCCURRENCE AND PETROGRAPHY

3.1 Occurrence

Thoeng basalt occurs as scattered masses of highly variable sizes and covers an area of approximately 85 km^2 (18% of the project area). Geographically, the basaltic terrain may be divided into four subareas, from north to south, as follows: Doi Dong Faen, Doi Kiu Saraeng, Ban Chiang Khian - Doi Kham and Doi Luang - Doi Pha Tang (Fig. 4). Among these subareas, basalts in the Ban Chiang Khian - Doi Kham are most voluminous and occupy an area of about 44 km^2, whereas those in the Doi Dong Faen, Doi Kiu Saraeng and Doi Luang - Doi Pha Tang cover areas of 10, 17 and 14 km^2, respectively.

The studied basaltic masses commonly form plateaux on the uppermost part of mountain range and commonly overlie the Upper Permian strata and the Permo-Triassic rocks. They are highly weathered and decomposed to brownish red soil; the fresh outcrops of these rocks are almost all restricted to the edges and slopes of mountain range (Fig. 5). These basaltic plateaux may once have occurred as a single plateau and subsequently have undergone erosion, leaving the remainder on the top of mountain range as seen in the present day.

Internal structures of individual Thoeng basaltic flows are similar to those of the typical subaerial basaltic flow, i.e. vesicular base, massive with platy and columnar joints at center (Fig. 6), and vesicular top, but for the fact that Thoeng basaltic flows are incomplete due to weathering and erosion. Platy and columnar joints have different attitudes, possibly due to paleotopography; the axes of columnar joints, and dip angles of platy joints are, however, largely almost vertical and horizontal, respectively. Vesicles in some flows are flattened parallel to platy joints, and Permo-Triassic tuff inclusions may be conspicuous. Thicknesses of some flows are up to greater than 10 m. Characteristics of some Thoeng basaltic flows are summarized in Table 1.

According to the high weathering and decomposition nature of Thoeng basalts, i.e. rock exposures are scarce and discontinuous, it is impossible to exactly determine the number of flows. On the basis of their internal structures and the scattered small outcrops along the slopes at different elevations in the north of Doi Dong Faen (southern side of a new road from Ban Mai Ya to Amphoe Wiang Chai), Thoeng basalts are estimated to be constituted by at least 5 flows. These flows have a total thickness of about 45 m (Chankaeo *et al.*, 1996; Mahatthanachai *et al.*, 1996; Lee-am *et al.*, 1996; Pongsaeree *et al.*, 1996; Thiankham *et al.*, 1996; and Chat-prasert *et al.*, 1996).

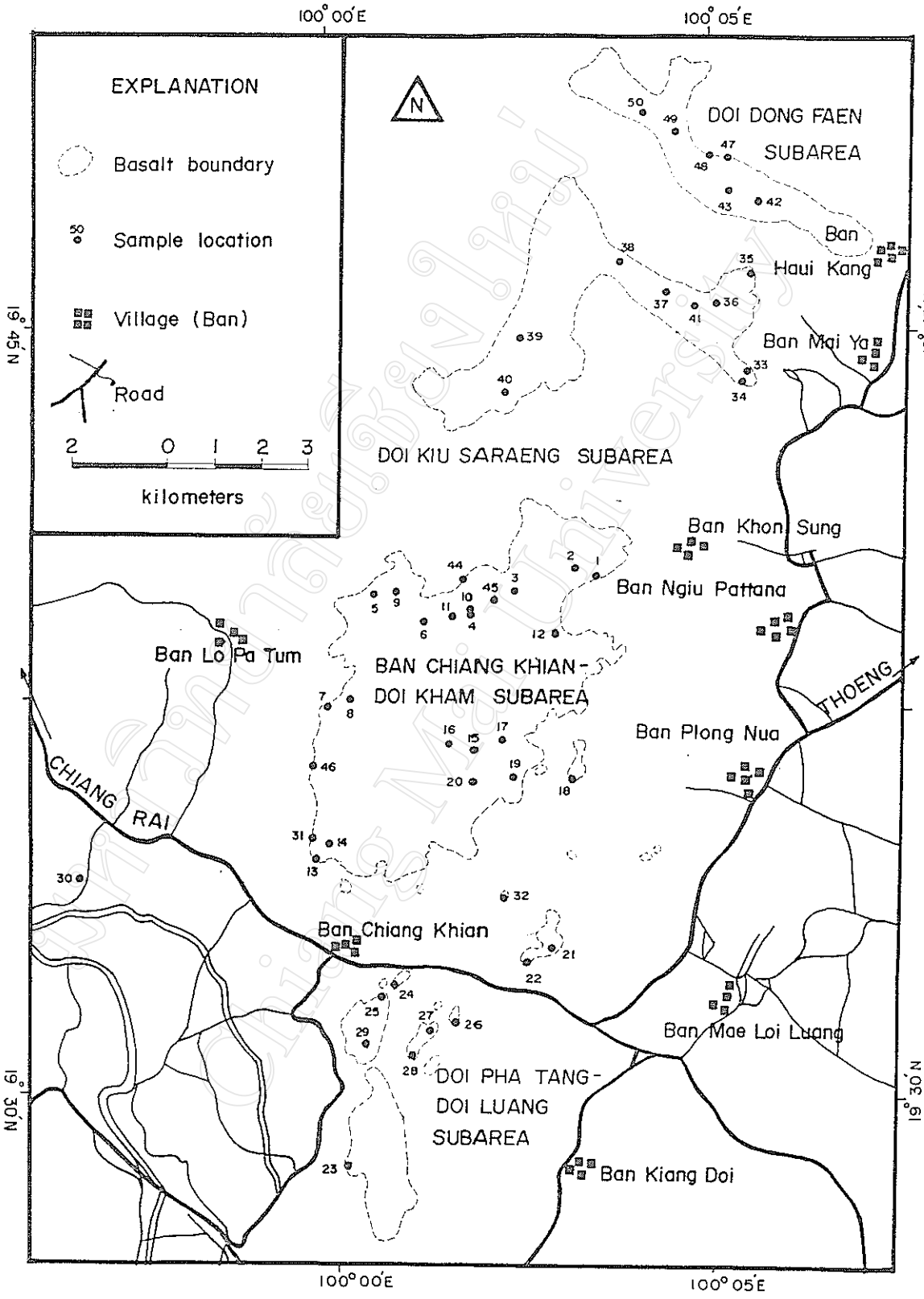

Figure 4 Map illustrating boundaries of Thoeng basalt in different subareas, and locations of samples presented in this study.

Figure 5 Outcrops of Thoeng basalts at grid references (a) 085776 and (b) 080774. Note that brownish red soil in both photos has been decomposed from basalts.

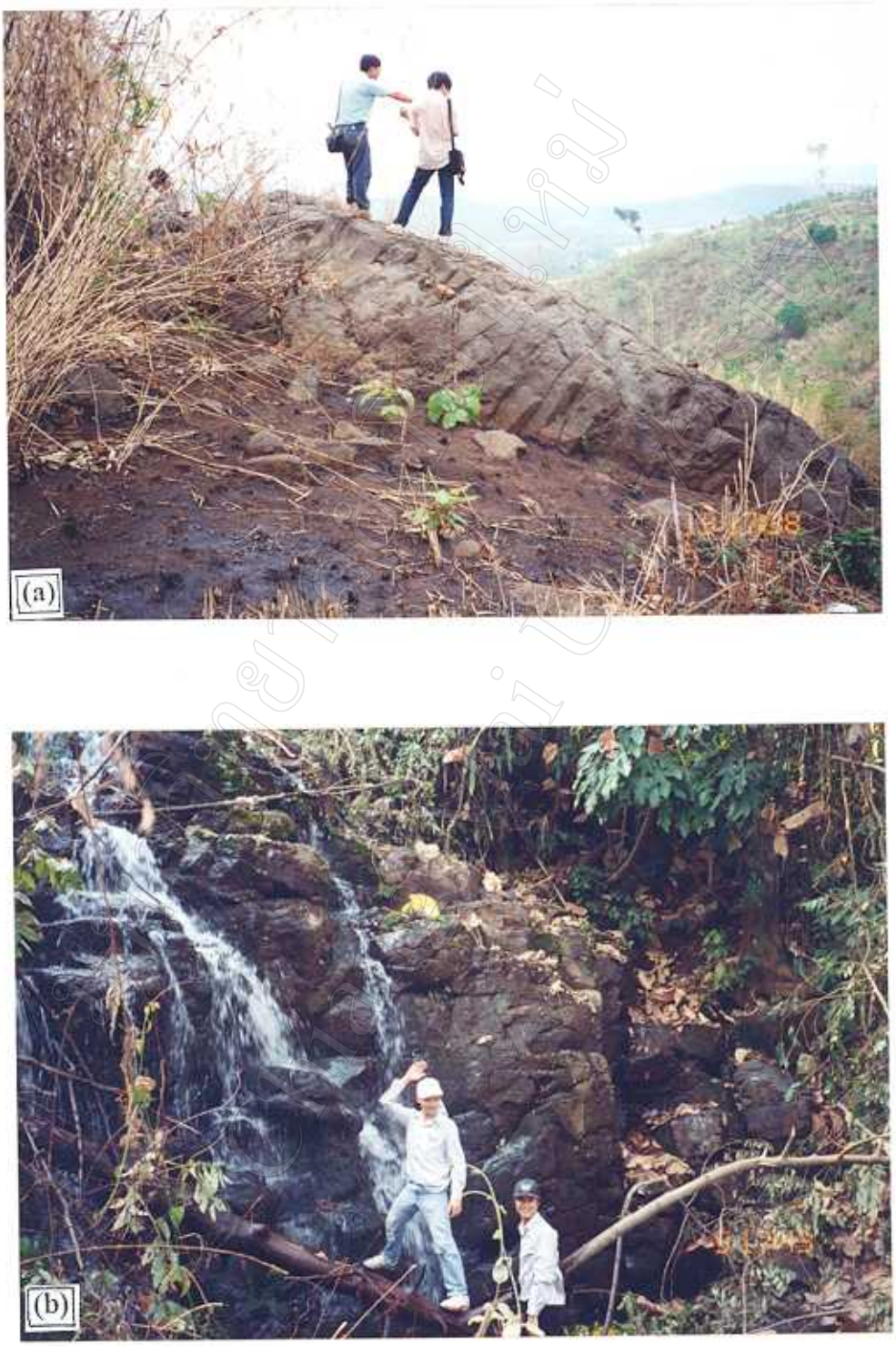

Figure 6 Exposures of Thoeng basalts showing (a) inclined columnar joints (grid reference 131846) and (b) platy joints (grid reference 085741).

Table 1 Outcrop locations, attitudes of platy and columnar joints, and thicknesses of individual flows of Thoeng basalt.

Grid reference	Plane of platy joint	Axis of columnar joint	Thickness of individual flow (m)	Remark
080774	-	30N55E	>2	Vesicular.
045751	-	-	>2	Massive and slightly vesicular, with flow bands.
079771	-	-	>3	Vesicular, vesicles flat
079774	-	-	>3	-tened in the direction normal to columnar joints.
085741	N71E 2NW	-	>8	Upper and middle por-
092742	-	-	>8	tions of flow.
103733	N5E 12NW	-	>5	Upper flow: upper part is vesicular, vesicles flattened parallel to platy joints; lower part is massive.
	N5E 12NW	-	>3	Lower flow: upper part is vesicular, vesicles flattened parallel to platy joints; lower part is massive and contains Permo-Triassic tuff xenoliths.
095734	N60W 50NE	-	>10	-
086704	-	-	>3	Underlain by Permo-Triassic tuff.
123848	-	72S80W	-	Slightly-moderately
131846				vesicular.

- = no data available.

3.2 Petrographic Study

Samples presented in this study were carefully selected to avoid, in general, rocks showing

(1) extensive development of mesoscopic domains of secondary minerals such as quartz resulted from silicification, epidote and chlorite,
(2) xenoliths other than basalt itself,
(3) abundant vesicles/amygdale minerals, and
(4) quartz, epidote or calcite veining or patches totalling more than approximately 5 modal%.

As a consequence, sixty-five basaltic samples are considered to be least-altered samples and may represent magma prior to eruption. Sample locations of the least-altered samples are given in Figure 4 and Appendix A.

These least-altered basaltic samples have been lithologically and petrographically studied. The results show that the Thoeng basalts have colors varying from dark grayish black to dark greenish black. They range texturally from slightly to strikingly megacrystic (Fig. 7); many are seriate-textured. Phenocryst and microphenocryst phases (sizes up to 2 cm across) generally include numerous plagioclase (Figs. 8, 9, 10, 11, 12, 13, 14, 15, 16, 17 and 18), subordinate olivine (Figs. 8, 10, 12, 13, 16, 17, 18, 19, 20, 21 and 24), and trace clinopyroxene (Figs. 8, 9, 10, 16 and 18) and Fe-Ti oxide; a few samples have olivine microphenocrysts dominated over plagioclase phenocrysts/microphenocrysts. In addition, megacrysts of Fe-Ti oxide (Figs. 10, 14 and 16), apatite (Fig. 22) and quartz (Fig. 23), and basaltic xenoliths have been sporadically detected in some samples. These phenocrysts/ microphenocrysts, megacrysts and xenoliths are embedded in the non-foliated, fine to very fine-grained groundmass that varies texturally from felty (Figs. 8, 9, 10, 11, 12, 13, 14, 16, 20 and 22) to trachytic (Figs. 18 and 23). Interstitial material may be primary ferromagnesian minerals (Fig. 8), glass (Fig. 18) and secondary calcites. Some samples are partly subophitic (Fig. 24) in addition to intergranular and intersertal fabrics. The holocrystalline basalts with subophitic relationship signify that they have undergone crystallization relatively slowly and may have occurred in the middle part of a thick flow. The hypocrystalline basalts with subophitic texture imply that while the rocks were cooling down relatively rapidly, there might have been another hot lava flow immediately overlying the partly solidified rock, resulting in relatively slow cooling rate in the underlying lava flow. The primary groundmass constituents are made up mainly of plagioclase laths with subordinate clinopyroxene and olivine, and minor Fe-Ti oxide minerals; many samples contain devitrified dark brown glass as a subordinate constituent. Amygdale and veinlets are rarely present. Amygdale minerals and fracture-infillings may be iron oxides/hydroxides, chlorite, calcite and zeolite. Petrographic features of individual samples are briefly presented in Appendix B.

Figure 7 Outcrops of (a) slightly porphyritic tholeiitic basalt at grid reference 067667, and (b) highly porphyritic basalt at grid reference 123848.

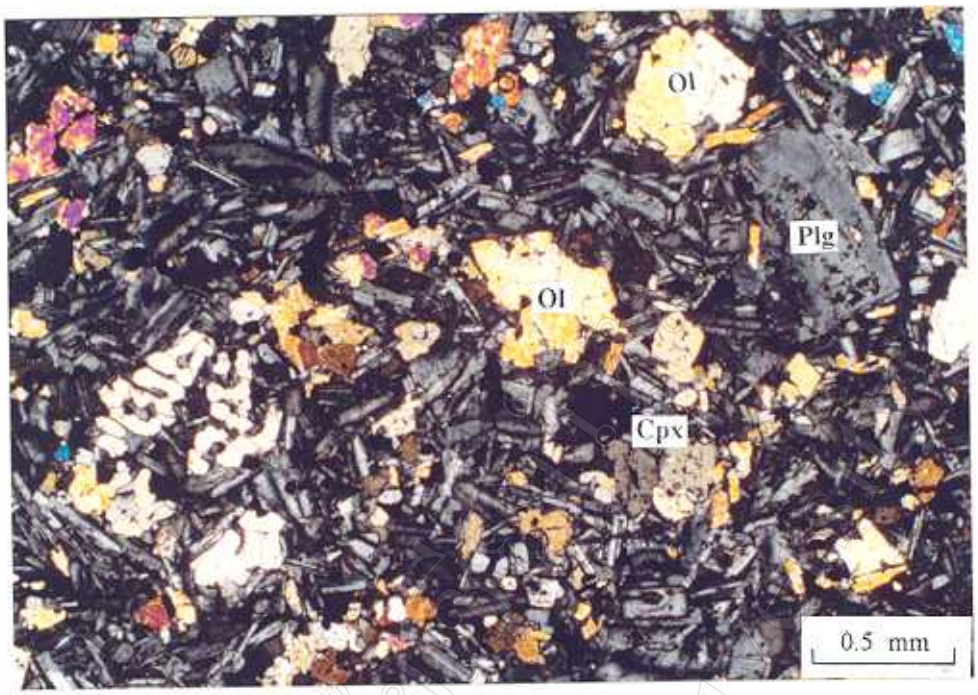

Figure 8 Photomicrograph of sample no. TB 19 displaying embayed and sieve-textured microphenocrysts of olivine (Ol), clinopyroxene (Cpx) and plagioclase (Plg) that are embedded in felted holocrystalline matrix. Crossed polars.

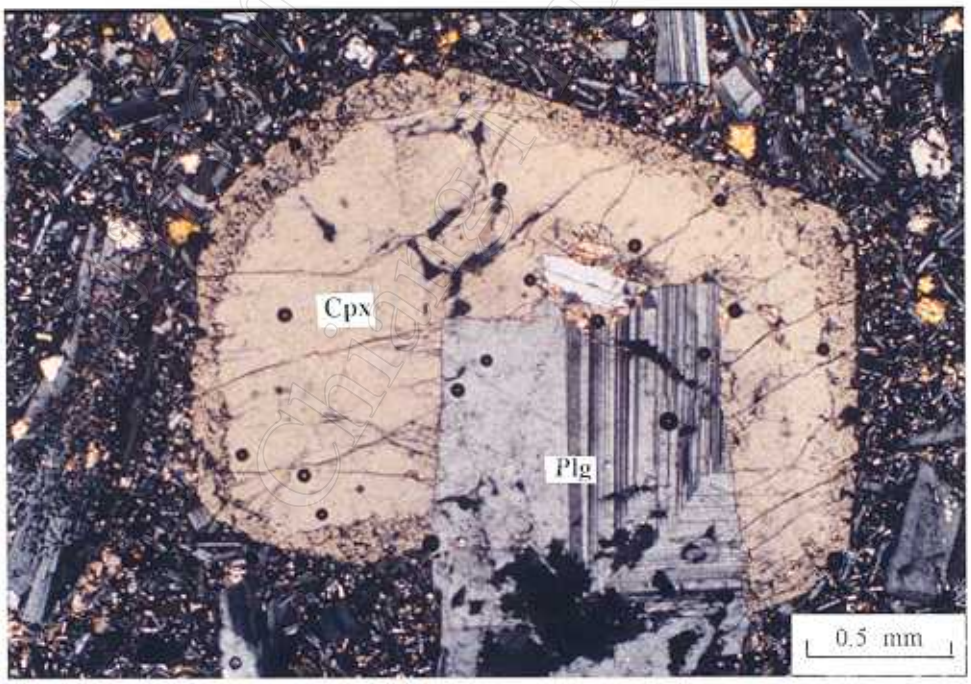

Figure 9 Photomicrograph of sample no. TB 31 illustrating clinopyroxene (Cpx) and plagioclase (Plg) phenocrysts. Note marginal resorption of clinopyroxene phenocrysts. Crossed polars.

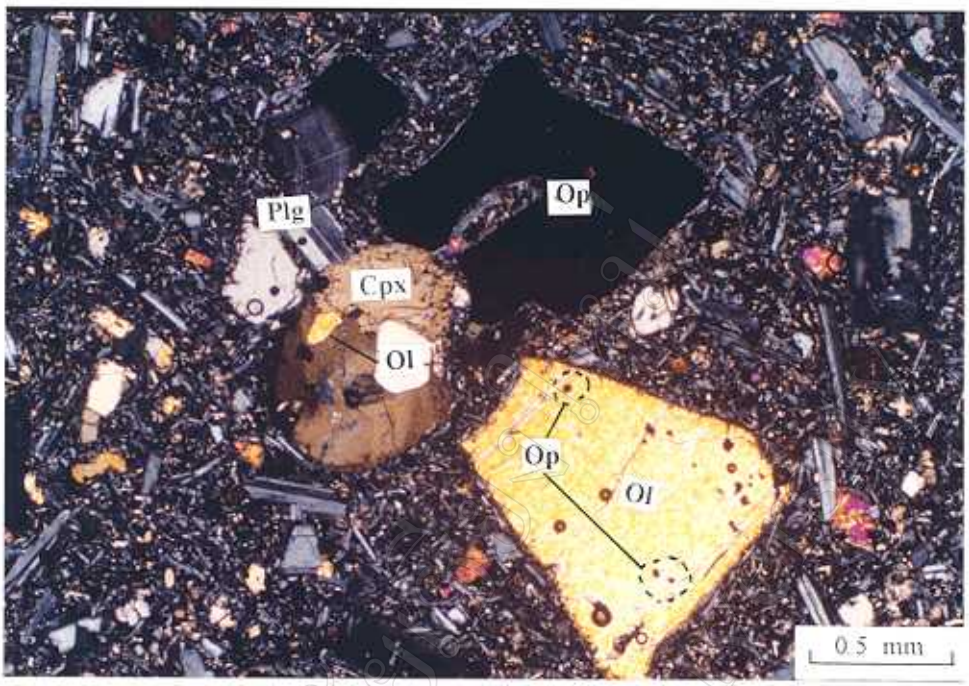

Figure 10 Photomicrograph of sample no. TB 31 displaying megacrysts of plagioclase (Plg), olivine (Ol), clinopyroxene (Cpx) and Fe-Ti oxide (Op). Note corroded features of these phases, secter zoning in clinopyroxene, and opaque (Op) (chrome-spinel/Fe-Ti oxide) inclusions in olivine. Crossed polars.

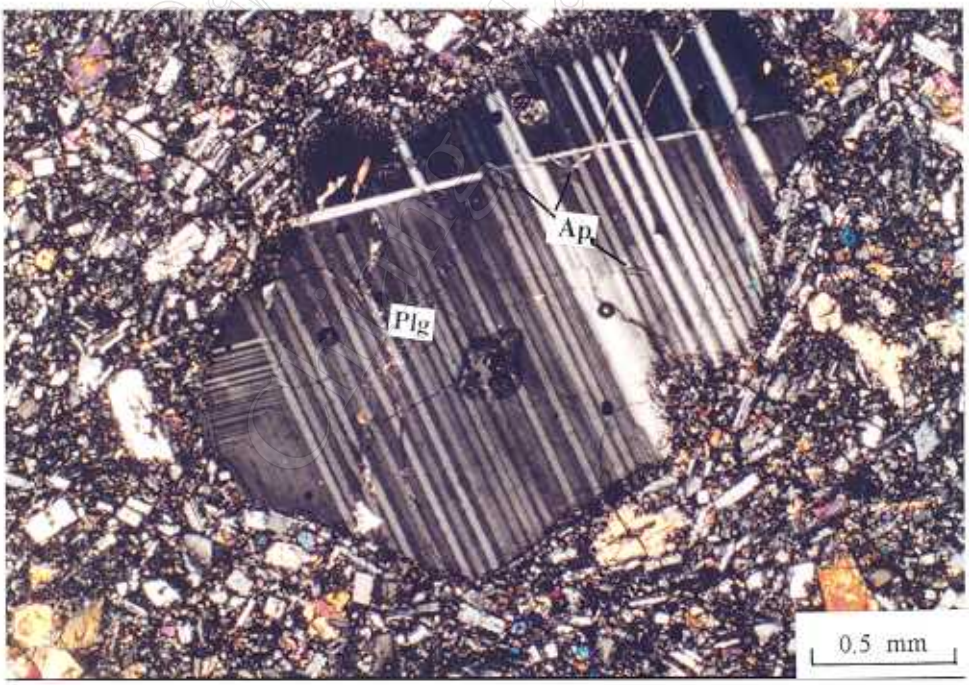

Figure 11 Photomicrograph of sample no. TB 32 showing small apatite (Ap) inclusions in corroded plagioclase (Plg) phenocryst. Crossed polars.

Figure 12 Photomicrograph of sample no. TB 1-6 showing isolated plagioclase and olivine microphenocrysts, plagioclase glomerocrysts with stellate fashion, and plagioclase - olivine cumulocryst (Plg = plagioclase, and Ol = olivine). Crossed polars.

Figure 13 Photomicrograph of sample no. TB 45 illustrating olivine (Ol) and sieve-textured plagioclase (Plg) microphenocrysts. Crossed polars.

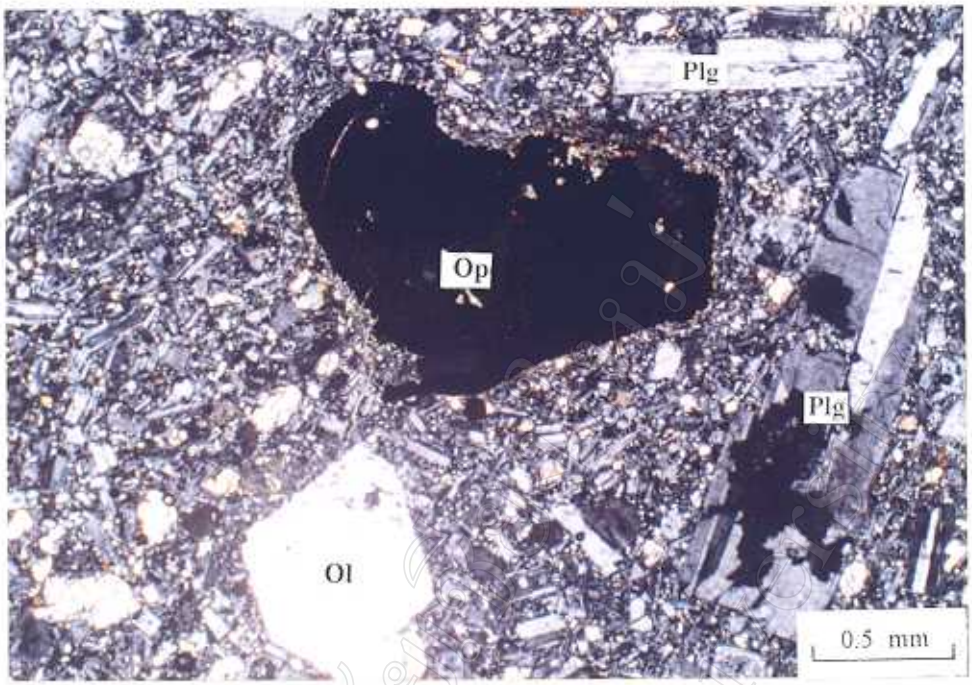

Figure 14 Photomicrograph of sample no. TB 2-2 showing anhedral Fe-Ti oxide (Op) megacryst, and euhedral plagioclase (Plg) and olivine (Ol) microphenocrysts. Crossed polars.

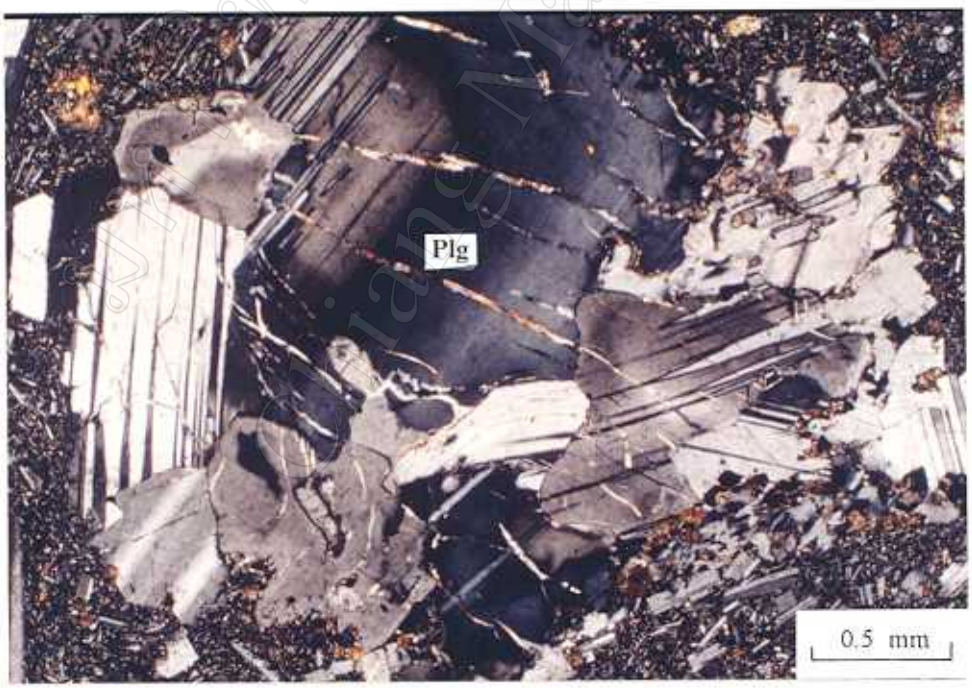

Figure 15 Photomicrograph of plagioclase (Plg) glomerocryst in sample no. TB 30. Crossed polars.

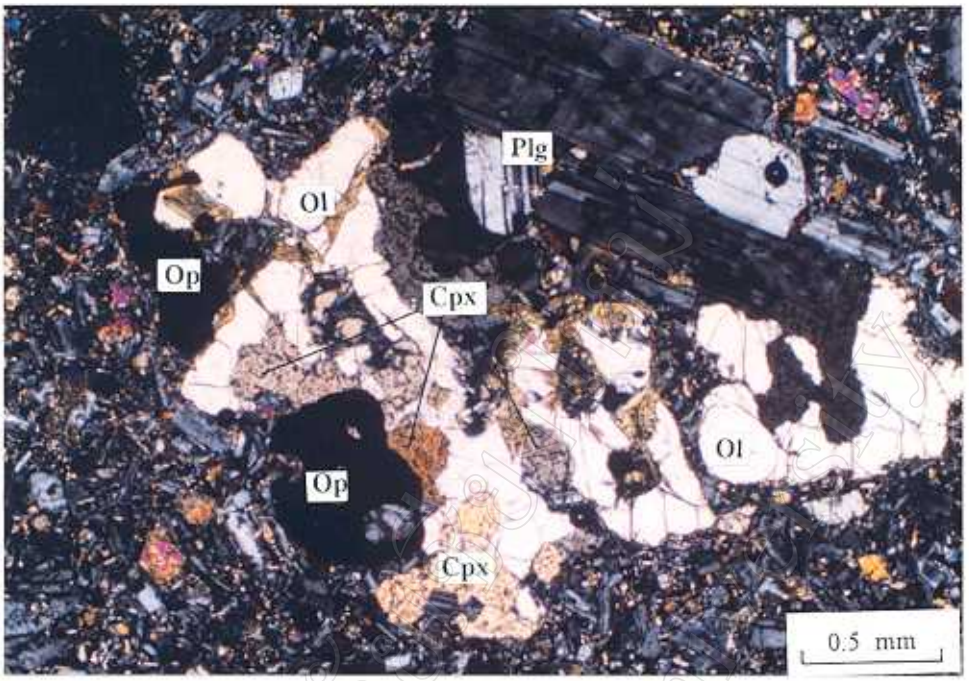

Figure 16 Photomicrograph of olivine (Ol) - clinopyroxene (Cpx) - Fe-Ti oxide (Op) cumulocryst, and plagioclase (Plg) phenocryst in sample no. T 3.1. Crossed polars.

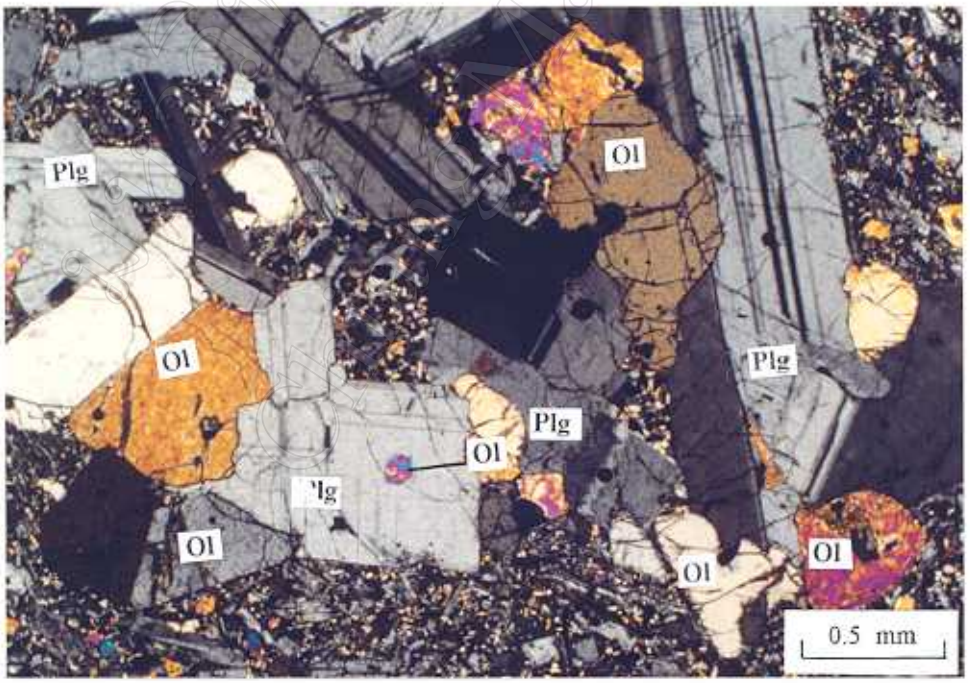

Figure 17 Photomicrograph of olivine (Ol) - plagioclase (Plg) cumulocryst in sample no. TB 23. Crossed polars.

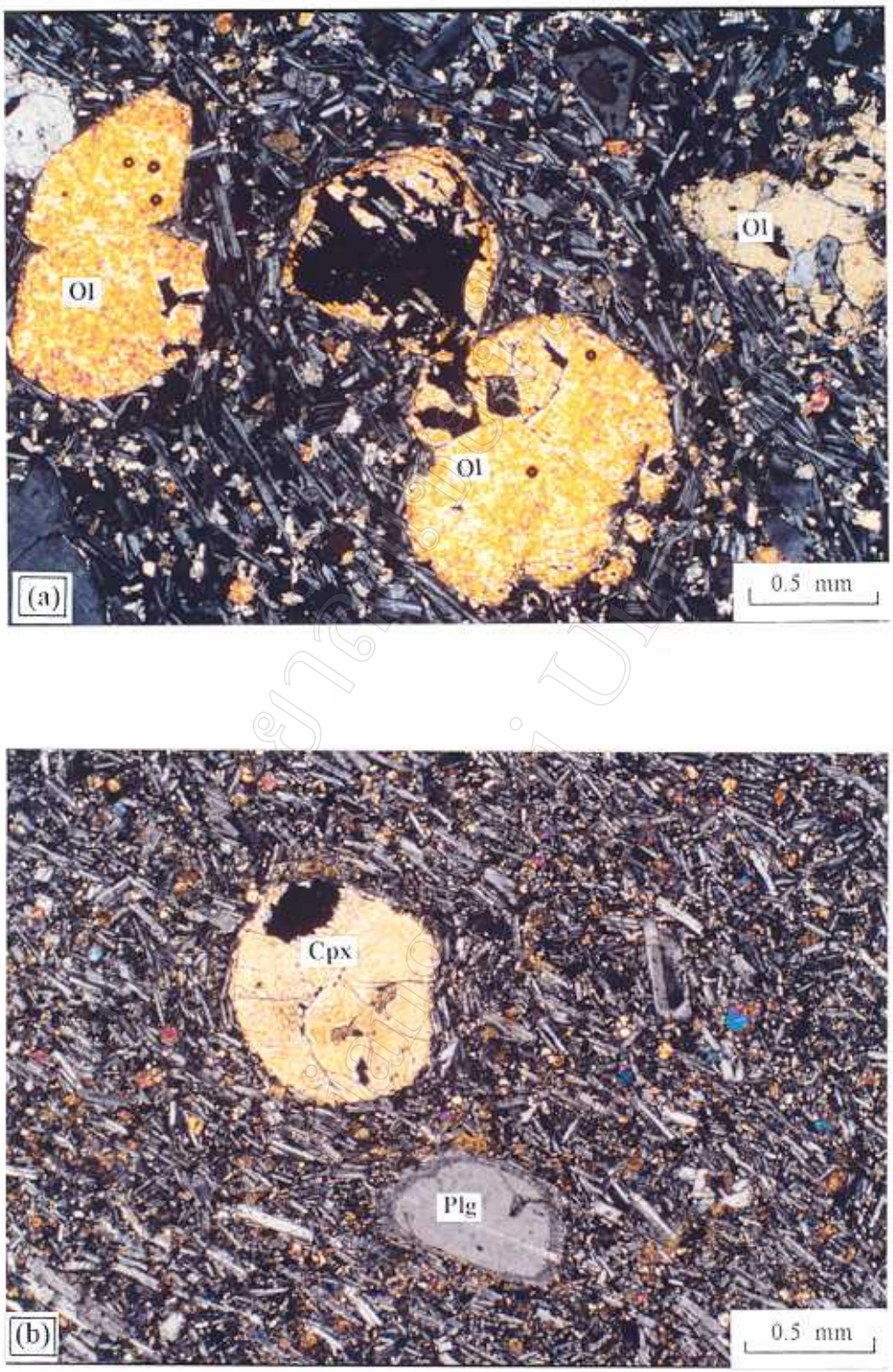

Figure 18 Photomicrographs showing (a) rounded olivine (Ol) phenocrysts/ microphenocrysts in hyalopilitic groundmass of sample no. TB 22, and (b) rounded plagioclase (Plg) and clinopyroxene (Cpx) phenocrysts/microphenocrysts in pilotaxitic groundmass of sample no. TB 27. Crossed polars.

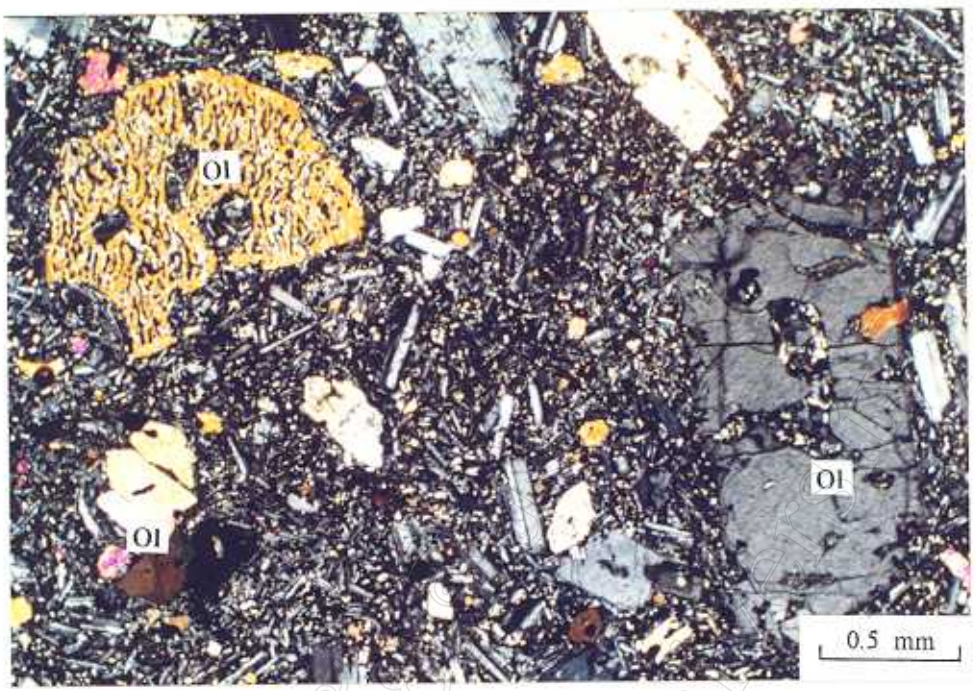

Figure 19 Photomicrograph of sample no. TB 50 displaying olivine (Ol) phenocrysts and microphenocrysts. Also shown are sieve texture and embayment in olivine phenocrysts. Crossed polars.

Figure 20 Photomicrograph of sample no. TB 41 displaying olivine (Ol) microphenocrysts in felted groundmass. Crossed polars.

Plagioclase phenocrysts/microphenocrysts commonly show anhedral to subhedral outlines with disequilibrium features, i.e. rounded edges (Figs. 8, 11, 13 and 18), embayment (Figs. 13 and 18) and sieve texture (Figs. 8, 13 and 18), zonal patterns (Fig. 15) and twins, and may have olivine, clinopyroxene, opaque and apatite inclusions (Fig. 11). Most of them occur as isolated crystals; a few may form stellate aggregates (Figs. 9), clots of sole plagioclase (glomerocrysts) as illustrated in Figures 12, 13 and 15, and clots of plagioclase, olivine and/or clinopyroxene (cumulocrysts) as shown in Figures. 9, 10, 16 and 17. Groundmass plagioclases are subhedral to anhedral, and may partially bear subophitic relationship to clinopyroxenes (Fig. 24). The alteration products of both phenocryst/microphenocryst and groundmass phases may be sericite, clay minerals, calcite, and iron oxides/hydroxides. The phenocrysts and microphenocrysts have experienced more extensive alteration relative to the groundmass phase.

Olivine phenocrysts and microphenocrysts have anhedral to euhedral (generally anhedral to subhedral) shapes. They commonly display sieve texture (Figs. 8, 19 and 21) and corroded outlines (Figs. 8, 10, 18 and 19), and may contain opaque (chrome-spinel or Fe-Ti oxide) and clinopyroxene inclusions. They occur as isolated crystals, glomerocrysts, and part of olivine ± plagioclase ± clinopyroxene cumulocrysts (Figs. 16 and 17); the former is predominant over the latter two. Groundmass olivines are almost all anhedral, and are intergranular to plagioclases. Olivines are moderately to highly replaced by chlorite/serpentine, iddingsite and iron oxides/hydroxides.

Clinopyroxene phenocrysts/microphenocrysts are euhedral to anhedral (mostly anhedral). They may occur as isolated crystals and as cumulocrysts, and contain plagioclase and opaque inclusions. Corroded and sieve features (Figs. 8, 9 and 10), and zoning are common. Groundmass clinopyroxenes mainly show anhedral to subhedral outlines and are commonly intergranular to plagioclases. Clinopyroxenes, both as phenocryst/microphenocryst and as groundmass phases, may be slightly replaced by chlorite and iron oxides/hydroxides.

Apatite megacrysts (sizes up to 1.5 mm across) are generally anhedral with rounded outlines, and occur as isolated crystals (Fig. 22). These megacrysts are very similar to those of Chiang Khong basanites that were misidentified to be corundum by Panjasawatwong and Youngsnong (1996). The presence of apatite megacrysts in Thoeng basalts is confirmed by Raman spectroscopy peaks as illustrated in Figure 25. According to Panjasawatwong and Youngsnong (1996), these megacrysts are interpreted to be xenocrysts derived from an unknown rock lying somewhere along the passage of ascending basaltic magma.

Fe-Ti oxide megacrysts are anhedral and have sizes up to about 0.5 mm across. They may occur as isolated crystals (Figs. 10 and 14) and part of cumulocrysts (Fig. 16). These megacrysts may be part of the xenolith which is made up at least of apatite and Fe-Ti oxide (Panjasawatwong and Youngsnong, 1996). Fe-

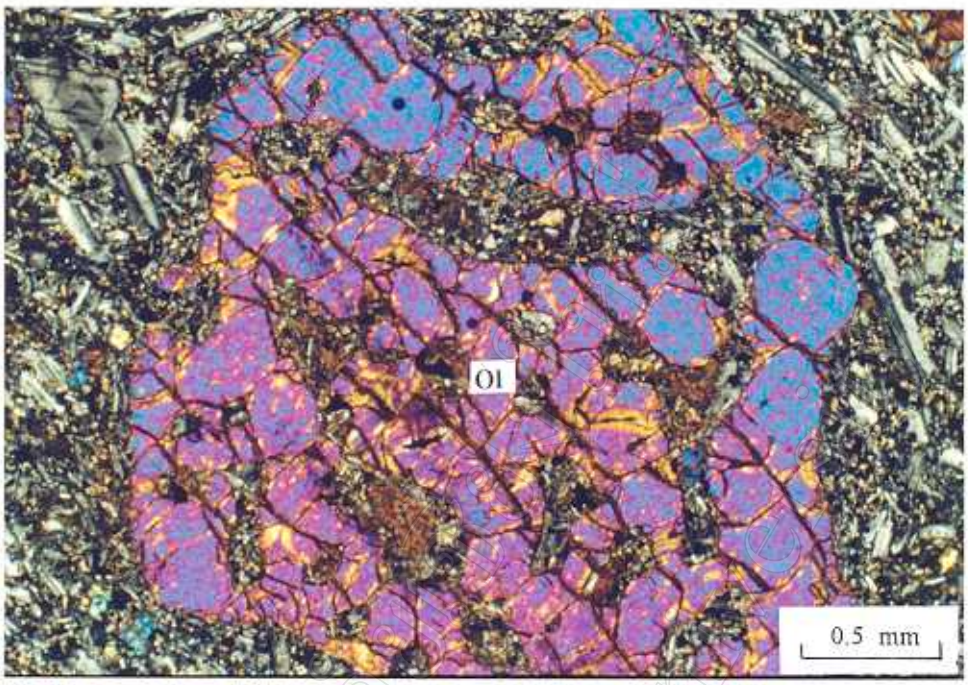

Figure 21 Photomicrograph of sieve-textured olivine phenocryst in sample no. TB 40. Crossed polars.

Figure 22 Photomicrograph of sample no. TB 32 showing rounded apatite (Ap) megacryst. Crossed polars.

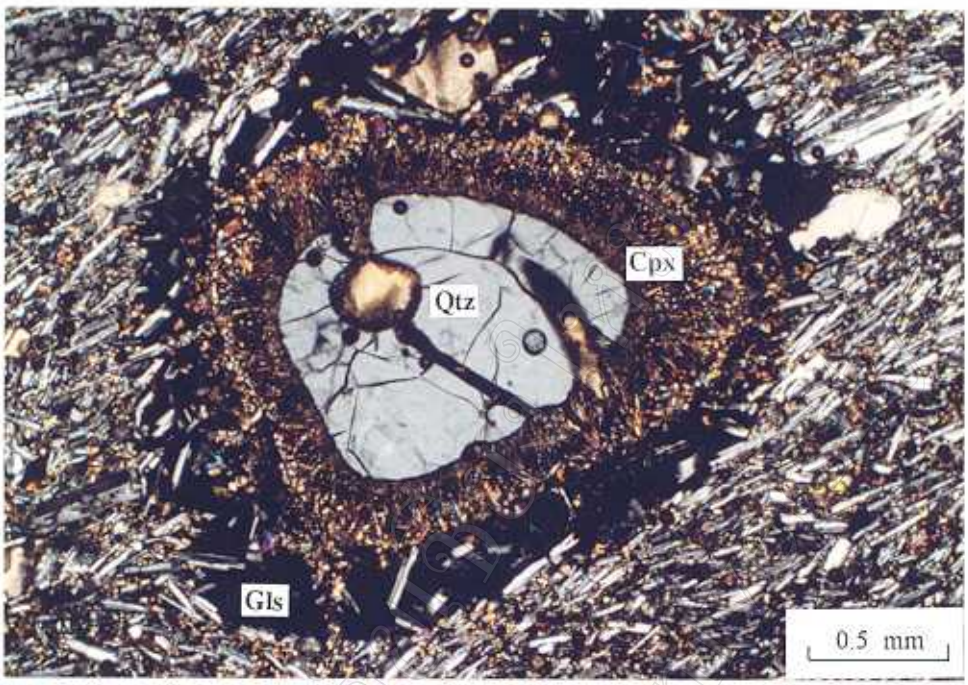

Figure 23 Photomicrograph of quartz (Qtz) megacryst with reaction corona in sample no. TB 25. Cpx = clinopyroxene, and Gls = glass. Crossed polars.

Figure 24 Photomicrographs showing subophitic textured groundmass in (a) sample no. TB 7 and (b) sample no. TB 47 (Plg = plagioclase, Cpx = clinopyroxene, and Ol = olivine). Crossed polars.

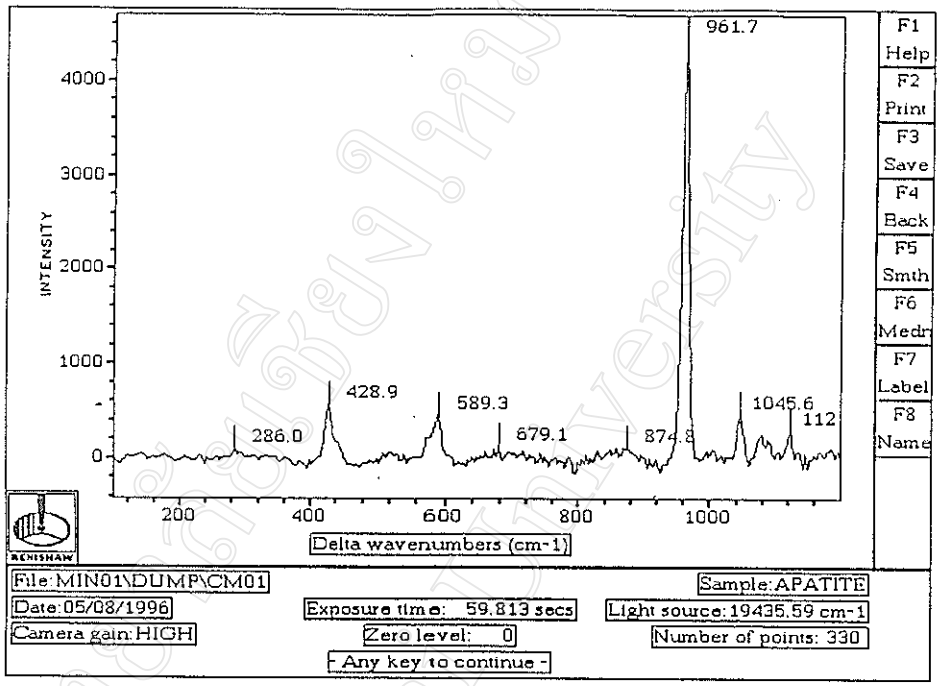

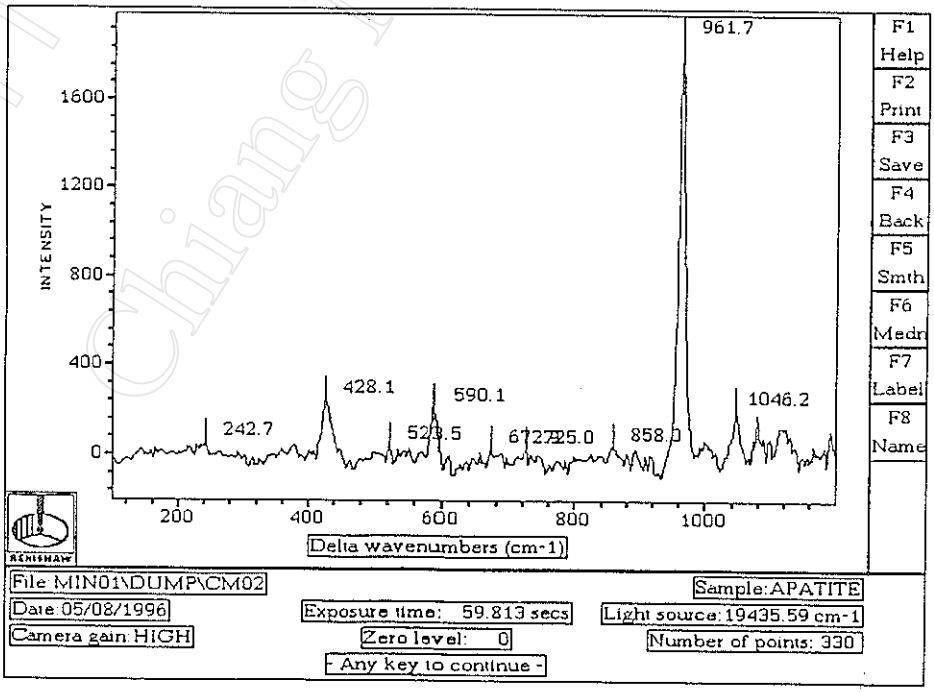

Figure 25 Raman spectrum peaks for two apatite megacrysts in sample no. TB 32.

Ti oxide microphenocrysts are euhedral to subhedral, and have sizes of groundmass minerals. Groundmass Fe-Ti oxide minerals occur as minute crystals with anhedral outlines. They are commonly associated with other interstitial minerals throughout the samples.

Quartz megacrysts, as indicated by Raman spectroscopy peaks in Figure 26a, are commonly mantled by acicular clinopyroxenes, in terms of reaction coronas, with glassy rinds, possibly resulted from quenching when cold quartz reacted with hot magma. Again, these are very identical to those found in Chiang Khong basanites that were assigned to be unknown minerals (Panjasawatwong and Youngsnong, 1996). These megacrysts are crustal xenocrysts incorporated into basalt during the uprising of basaltic magma. The clinopyroxene mantle is identified to be diopside by Raman spectroscopy technique (Fig. 26b).

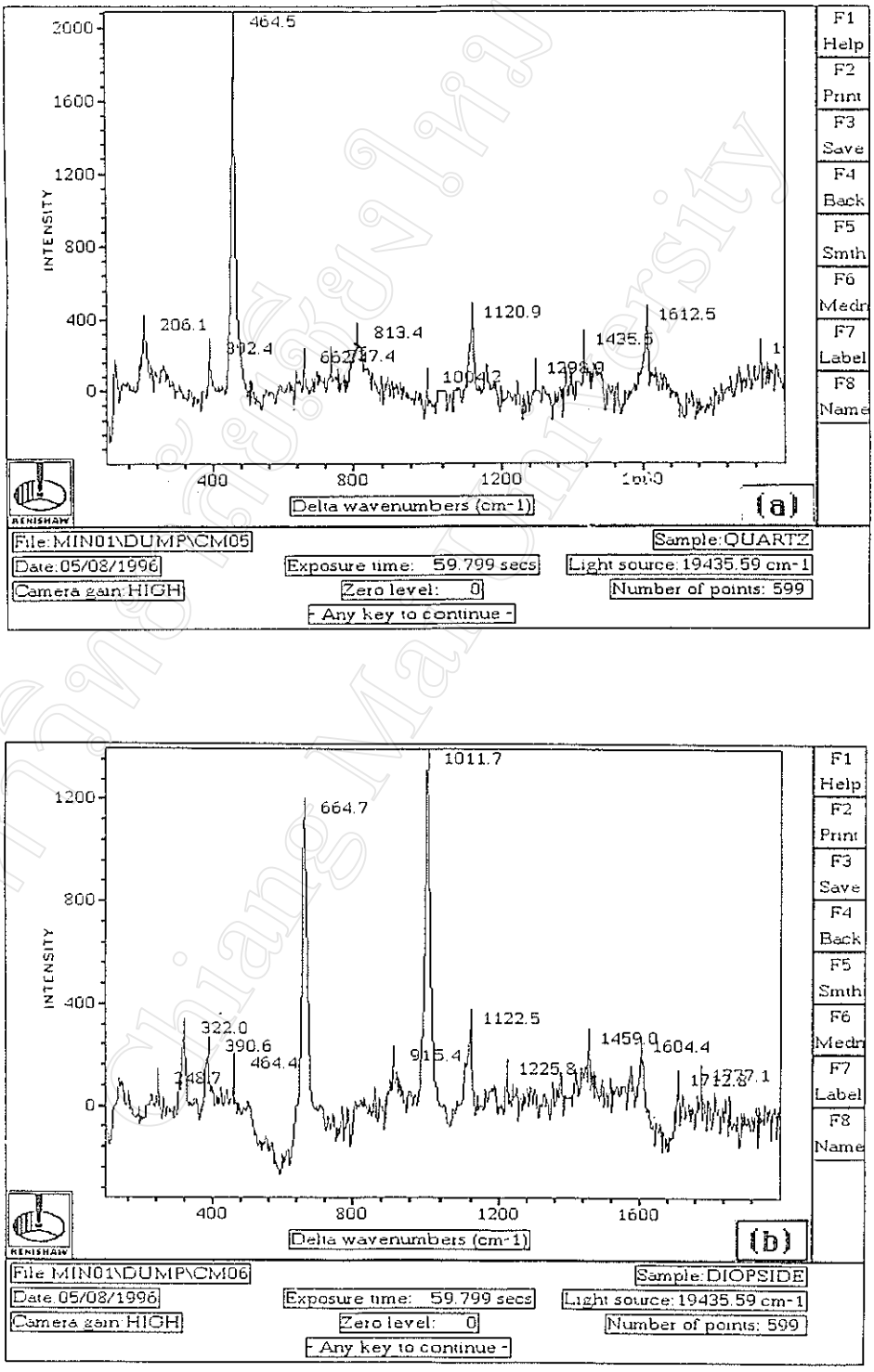

Figure 26 Raman spectrum peaks for (a) quartz megacryst, and (b) diopside, which is acicular, and borders the quartz megacryst as reaction rim, in sample no. TB 32.